Optical flow velocimetry inside an entrained cavity

Alecsandra Rambert, Afif Elcafsi, Pierre Gougat*

* LIMSI-CNRS, B.P. 133, 91403 Orsay, France

ABSTRACT

A number of studies have referred to the existence of a vortex cell within an urban street canyon when ambient winds aloft are perpendicular to the street. The understanding of vortex dynamics or vorticity distribution in a such configuration is of great interest. Vortex structures play an important role in the dynamics of pollutant dispersion. This configuration was simulated by the interaction between a boundary layer and a cavity. Experimental characterisation of the vortex structures evolution was developed by flow velocity measurements inside and out of the cavity. Classical methods like hot wire and Laser Doppler Velocimetry (LDV) display only local measurements. Particle Image Velocimetry (PIV) method is based on the optical flow technique developed by G. Quénot (1992). Optical flow computation consists in extracting a dense velocity field from an image sequence assuming that the intensity is conserved during the displacement. Compared with the classical DPIV method, this technique has the following advantages: (i) it can be applied simultaneously to sequences of more than two images; (ii) it performs a global image match by enforcing continuity and regularity constrains on the flow field. This helps in ambiguous or low particle density regions; (iii) It provides dense velocity fields (neither holes nor border offsets); (v) local correlation is iteratively searched for in regions whose shape is modified by the flow, instead of being searched by fixed windows. This greatly improves the accuracy in regions with strong velocity gradients.

An approach Large Eddies Simulation was developed to characterise the flow vortex structures in the cavity . The experimental results obtained by PIV based on optical flow are used in order to valid the numerical model. This technique emphasis the vortex structures inside the cavity which present small scales as well as large scales related to the cavity geometry. Theses vortices are usually non-stationary.

INTRODUCTION

For a urban pollution study it is essential to estimate qualitatively and quantitatively the pollutant concentrations and their spatial and time evolution which is strongly connected to the flow movements in this region. The majority of recent studies of circulation in street canyon have been performed by physical and numerical simulations. Physical simulation studies concerned pollutant levels in street canyons under various geometries show increases of concentration predicted consistent with a vortex flow pattern (Wedding et al., 1977). Much attention has been directed to the study of the various canyon flow regimes (DePaul and Sheih, 1986) since air flow is responsible for the transport of pollutants. Canyon geometry is an important determinant of characteristic airflow observed within urban canyons. Previous studies used a k-ε turbulence model of air flow to confirm the wind tunnels observations. The model was based on that developed by (Paterson and Apelt, 1989) to predict pressure experienced by walls of buildings within cities. It solves the Navier-Stokes equations for momentum and the equations for the transportation and dissipation of turbulent kinetic energy.

The interaction between a boundary layer and a street canyon was simulated by a forced flow past a cavity. In order to characterise the large unsteady vortices that take place in a such configuration we have developed an experimental set-up and associated measurement techniques which permit to realise local and global velocity measurements. In parallel with the experimental study a numerical work was developed in order to characterise the spatial and time dependant flow pattern in a boundary layer-cavity interaction. for the same geometrical and hydrodynamic conditions. To this aim the Large Eddy Simulation approach was chosen with a specific subgrid viscosity model which has been implemented in different algorithms for the integration of the Navier-Stokes equations.

The numerical and experimental quantitative prediction of the vortex flow in this configuration remains still approximate so we decided to study a simplified configuration represented by the interaction between a laminar boundary layer and a cavity.

MATERIAL AND METHODS

The experimental set-up is presented in Fig. 1. The cavity characteristic dimensions are indicated in meters in Table 1 were H is the height, L the length and l the width of the cavity.

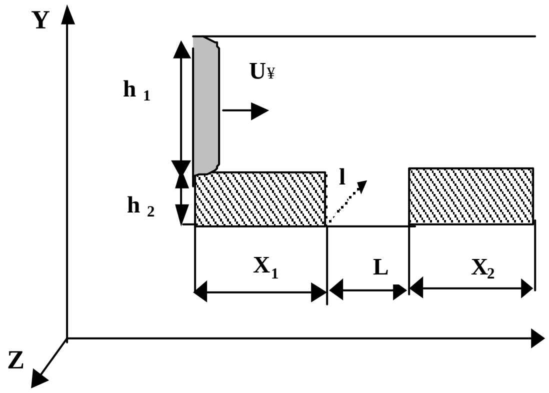

Fig.1 Geometrical configuration

h_1	h_2	l	L	X_1	X_2
0.07	0.05	0.03	0.1	0.2	0.3

Table 1 Characteristic dimensions of the cavity

Velocity profiles in the boundary layer were obtained by hot wire measurements. The interaction region between the boundary layer and the cavity and the vortex burst from the cavity were characterised by Laser Doppler Velocimetry measurements. The flow inside the cavity was characterised using Particle Image Velocimetry based on Optical Flow. The optical flow method offers a new approach for analysing flow images. It largely improves spatial accuracy and minimises the number of spurious vectors. Optical flow computation consists in extracting a dense velocity field from an image sequence assuming that the intensity is conserved during the displacement. Several techniques have been developed for the computation of optical flow. The technique that was chosen for PIV application was introduced by Quénot (1999) as Orthogonal Dynamic Programming algorithm for optical flow detection from a pair of images. Compared with the classical PIV method, the optical flow has the following advantages: (i) it can be applied simultaneously to sequences of more than two images; (ii) it performs a global image match by enforcing continuity and regularity constrains on the flow field. This helps in ambiguous or low particle density regions; (iii) It provides dense velocity fields (iiii) local correlation is iteratively searched for in regions whose shape is modified by the flow, instead of being searched by fixed windows. This greatly improves the accuracy in regions with strong velocity gradients.

A sequence of 50 images was recorded by a digital camera of 30 images/s (Pulnix 9701). The time between two images is 1.5 ms. Lens magnification is 0.16. *Lycopodium* particles and smoke were used as seeding.

Measurements were performed for different mean velocities and for different cavity shape ratio (h_2/L) obtained by changing the h_2 dimension and keeping the length L constant or by changing the L dimension and keeping the cavity height h_2 constant.

In order to investigate the three dimensional flow pattern developed in this configuration, measurement were also performed by PIV in a perpendicular plane of the flow, in the central region of the cavity.

RESULTS

At the entry of the cavity the boundary layer is laminar and is matching with a Blasius profile (η versus U/U_∞, $\eta = \frac{U_\infty y}{\sqrt{Re_x}}$). The mean velocity histogram obtained by Laser Doppler Velocimetry at $X=X_1$ and $h=h_1/2$ is presented on Fig. 2a (U_∞ equal to 1.4 m/s $Rex=1.6\times10^4$). The corresponding velocity profile obtained by hot wire measurements is presented in Fig. 2b.

Measurements made after the cavity showed that the initial laminar profile was modified. In Fig. 2c we presented the velocity profiles obtained after the cavity at x=310. A quantitative analysis of the velocity profiles after the cavity was made in terms of the boundary layer thickness: thickness δ, displacement thickness $\delta 1$ and momentum thickness $\delta 2$. The experimental results were compared with the classical formulas corresponding to a turbulent boundary layer (logarithmic profile):

$$\delta = \frac{0.38X}{Re^{0.2}{}_x}; \ \delta_1 = \frac{0.045X}{Re^{0.2}{}_x}; \ \delta_2 = \frac{0.037X}{Re^{0.2}{}_x}$$

The results are presented In Table 2 for x=310 mm. One can see that the turbulent regime is not established. The velocity profile presented on Fig. 2c is the result of the flow interaction with the cavity.

u (m/s)	**delta (m)**		**delta1 (m)**		**delta 2 (m)**	
	exp	**turbulent**	**exp**	**turbulent**	**exp**	**turbulent**
1.2	1.58E-02	1.73E-02	2.82E-03	2.17E-03	1.00E-03	1.69E-03
3	1.40E-02	1.45E-02	1.87E-03	1.82E-03	1.44E-03	1.42E-03
5	1.60E-02	1.32E-02	2.10E-03	1.66E-03	1.64E-03	1.29E-03

Table 2: Comparison of boundary layer characteristics (thickness) for experimental data and a turbulent logarithmic profile

Number

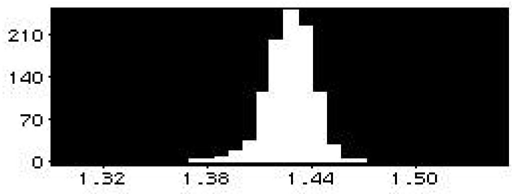

Velocity (m/s)

Fig. 2a
Mean velocity histogram

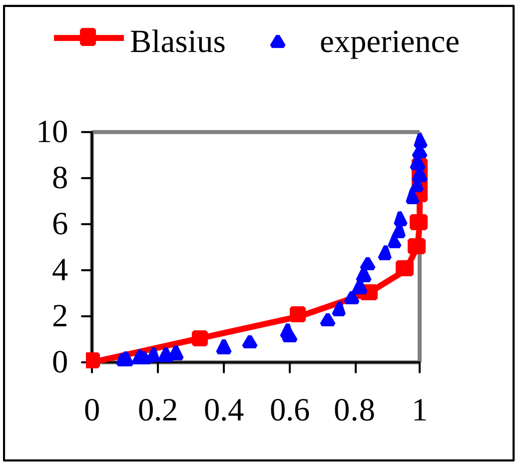

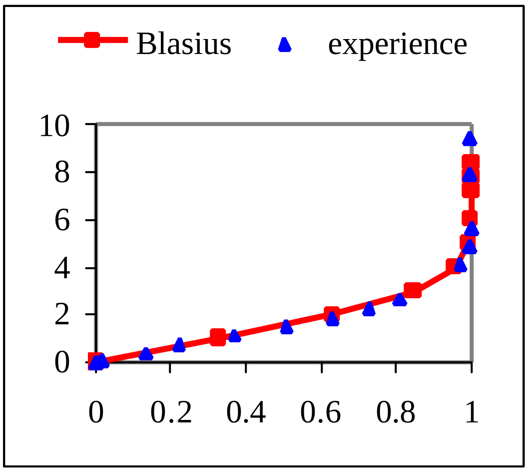

Fig. 2b

Fig. 2c

(2b) before the cavity (x=200 mm) (2c) after the cavity (x=310 mm)
Fig. 2 Mean velocity and velocity profiles in boundary layer

A visualisation realised in this region (x=300 mm, y=50mm) for a mean velocity of 1.2 m/s points out the presence of vortex structures coming out from the cavity and their movement (Fig. 3).

Fig. 3 Smoke visualisation of vortex release from the cavity

Knowing the time between images and the magnification one can estimate the mean translation velocity of the vortex structure which is sensibly the same as the mean velocity flow. At the same location, measurements performed by LDV furnish quantitative information about the vortex structures as mean velocity and frequency.

Measurements performed by LDV inside the cavity (Figure 4) show negative values of the velocity significant of the vortices presence in this region. The measurements were performed during 1.6 seconds.

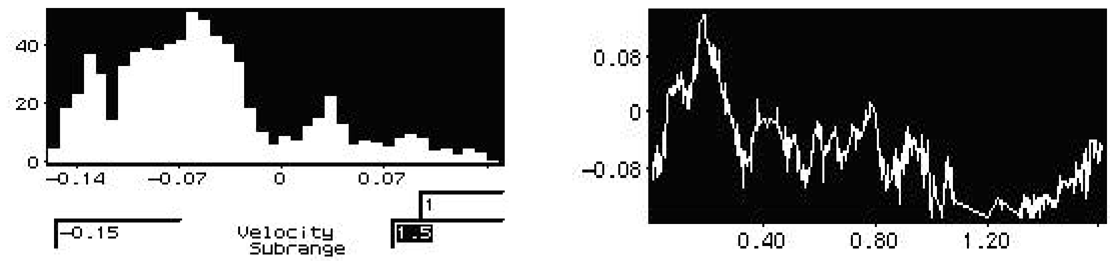

Fig 4a. Velocity histogram and time evolution inside the cavity in point A (x=260 mm, y=25 mm)

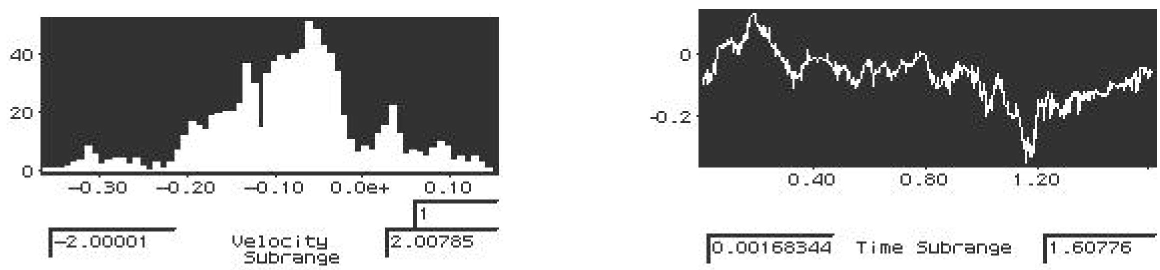

Fig 4b. Velocity histogram and time evolution inside the cavity in point B (x=270 mm, y=25 mm)

Fig. 4 Velocity histogram and time evolution inside the cavity

We can see that the mean velocity in point B is about twice the mean velocity in A which characterises a vortex region of a higher intensity. The Rms values are about 0.09 m/s and 0.05 m/s, respectively. The time dependence show the unsteady character of the flow inside the cavity. A spectral analysis of the velocity signal gives the characteristic frequencies of the flow in this region. The frequency values obtained in point B are less then 5 Hz (Figure 5a). A numerical result is presented on Figure 5b obtained for the same configuration and at the same location.

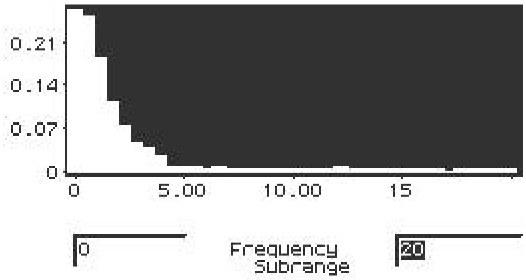

Fig.5a

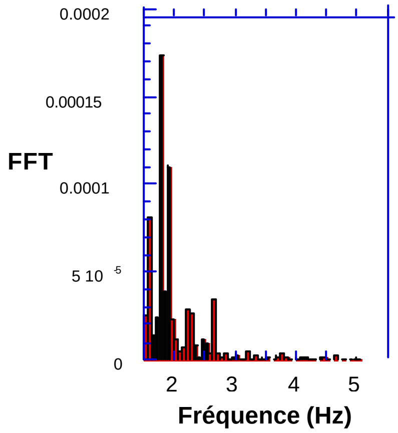

Fig. 5b

Fig. 5 FFT power density obtained at x=250 mm y=25 mm obtained by LDV measurements (Fig. 5a) and by LES simulation (Fig. 5b)

Figure 6a shows an example of velocity histogram and its time dependence obtained at x=310mm y=75 mm, after the cavity in the vortex escape region. The auto-correlation analysis of the signal (Fig. 6b) permitted to identify a characteristic frequency about 17 Hz.

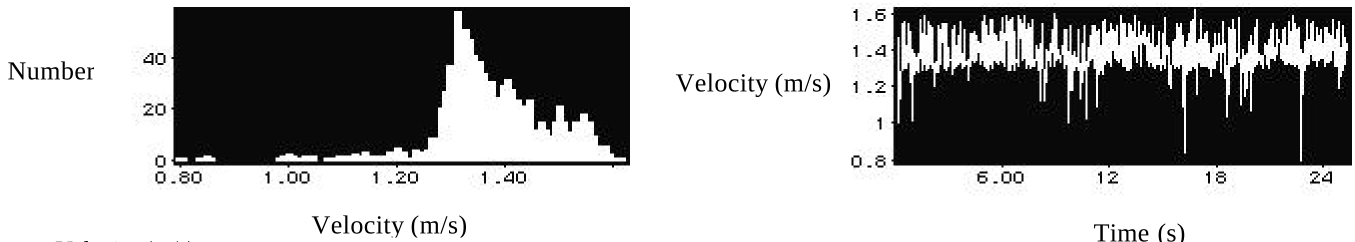

Velocity (m/s)

FFT power

Fig. 6a Velocity histogram and its time dependence (x=310 mm y=75mm)

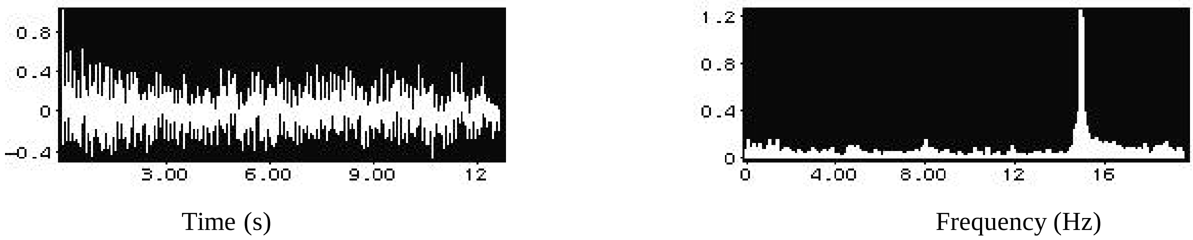

Fig. 6b Velocity autocorrelation signal and FFT power density (x=310 mm y=75mm)

Measurements were performed for different cavity shape ratio and for different mean velocities. The different shape ratio was obtained by (i) changing the height of the cavity h_2 and keeping the length L constant and (ii) by changing the length L of the cavity and keeping the height h_2 constant. The results of the vortex escape frequency corresponding to these cases are presented in Figure 7a and Figure 7b as a function of the adimensional factors U/h_2 and U/L, respectively.

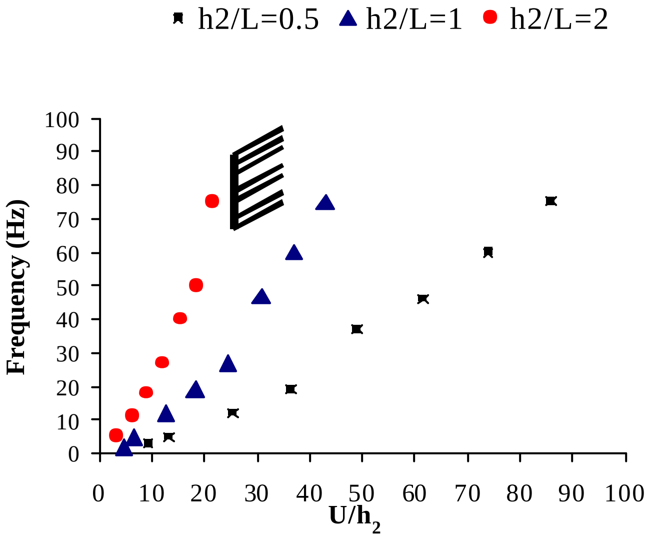

Fig. 7a Vortex frequency as a function of U/h_2 for different cavities shape ratio $h_2/L_{|L=constant}$

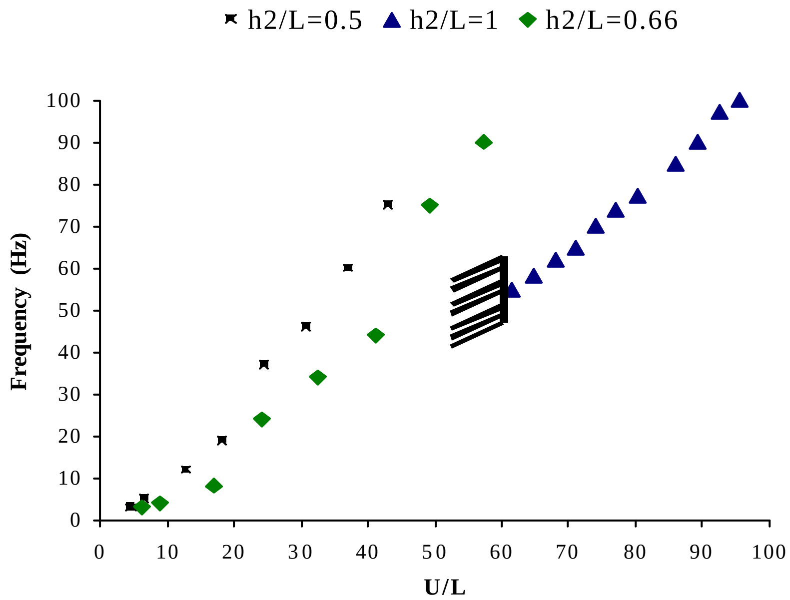

Fig. 7b Vortex frequency as a function of U/L for different cavities shape ratio $h_2/L_{|h2= constant}$

The vortex escape depends on the manner that the shape ratio was obtained, by changing the h_2 or the L cavity characteristic dimensions. For the shape ratio $h_2/L|_{h2=constant}$ and $h_2/L|_{L=constant}$ equal to 0.5 and for the same velocities, there is no difference between the vortex escape frequencies. We notice that for the shape ratio $h_2/L|_{h2=constant}$ equal to 1 there is no vortex escape for a mean velocity less then 3 m/s. The frequencies performed in this case are sensibly greater then those obtained for the same shape factor $h_2/L|_{L=constant}$. For the case of a shape ratio $h_2/L|_{L=constant}$ equal to 2 there is no vortex escape for a mean velocity more then 4 m/s. Measurements made for $h_2/L|_{h2=constant}$ equal to 2 showed that there is not vortex escape at all for any mean velocity value.

Comparing the vortex escape frequencies for the same velocities for different $h_2/L|_{L=constant}$ values we notice that this shape factor has not a significant influence on the vortex escape behaviour. On the contrary, analysing the results obtained for the $h_2/L|_{h2=constant}$ case we conclude that the length L of the cavity is a characteristic dimension which plays an important role in the vortex escape phenomenon.

For the same aerodynamic conditions and geometrical configuration a LES (Large Eddy Simulation) numerical code was developed (Chabni, 1997). At the entry of the cavity the numerical velocity profile matches with Blasius profile. An analysis of the numerical velocity signal corresponding to x=310 mm and y=75 mm points out a characteristic frequency about 17 Hz which agrees well with the experimental results (Fig. 8). The numerical code will be tested for other different Reynolds numbers in order to compare the numerical results with the experimental ones.

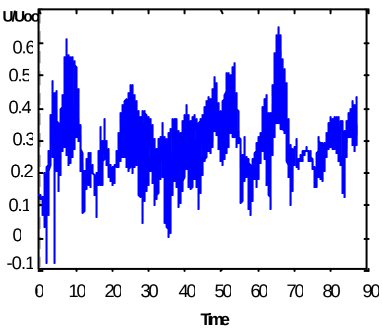

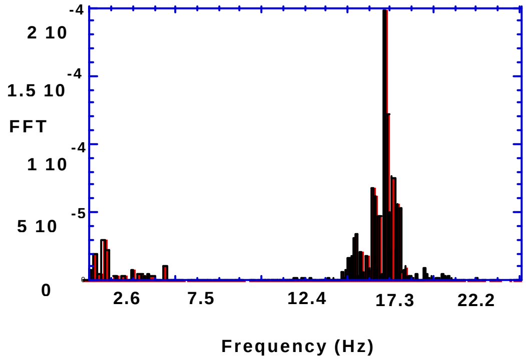

Fig 8 Numerical velocity time dependence and FFT density power

To improve the characterisation of the vortex structures global velocity measurements were performed by PIV based on optical flow inside the cavity. An example of such a velocity field is presented in Fig. 9.

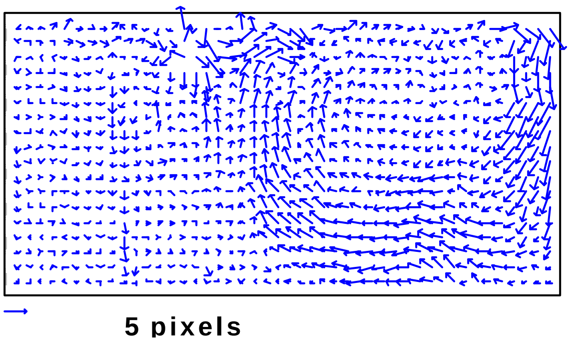

Fig. 9 Flow velocity fields obtained inside the cavity

Two counter rotating vortex are observed with eddies of smaller dimensions turning around them. The vortex has a diameter equal to the height of the cavity. The velocity inside the cavity is about 0.2--0.3 m/s. An analysis of the vector map show that in the right region of the cavity the vortex intensity is higher, result which agrees well with the LDV measurements performed in the same regions. In order to better characterise the movement of the main vortex, measurements were performed only in the right side of the cavity (Fig. 10).

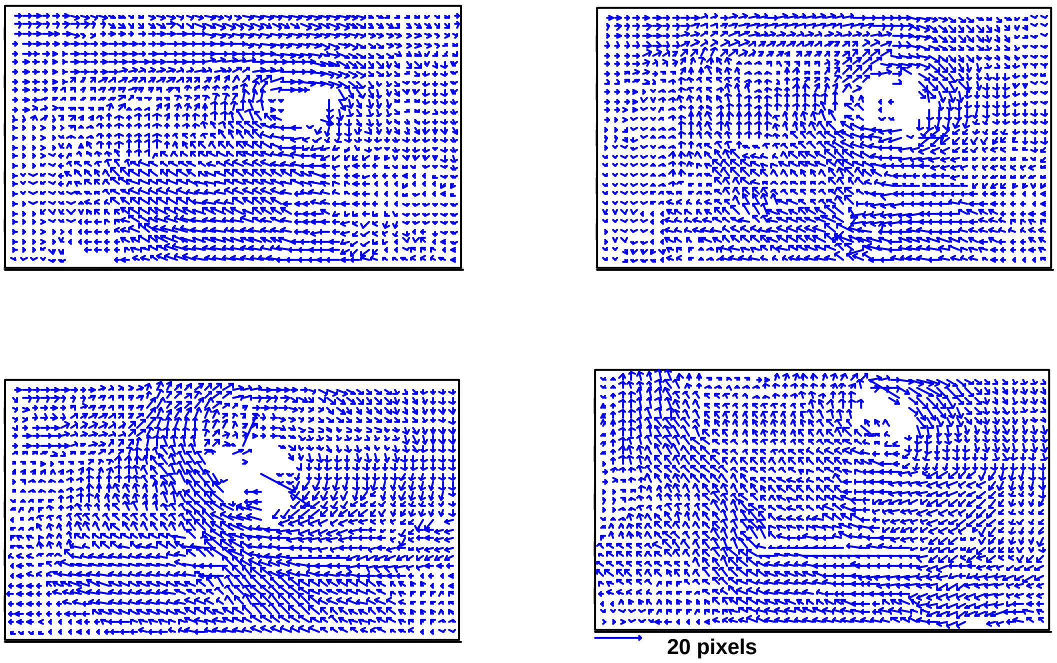

Fig. 10 Time evolution of instantaneous velocity fields (time between fields is 66 ms)

Time between two velocity fields is 66ms. Due to the viscous effects this structure entrains the environmental fluid and its diameter growths. We can identify an ascension movement in order to burst out from the cavity.

CONCLUSION

The main application of this work is the study of the pollutant transport and dispersion in a canyon street. The study of the interaction between a boundary layer and a cavity is a first approach in characterisation of flow regimes within the urban canyon.

The movement dynamics was characterised by local (Laser Doppler Velocimetry) and global velocity measurements (Particle Image Velocimetry). Laser Doppler Velocimetry measurements furnish information about the time evolution of the fluid velocity. Vortex release characteristic frequencies were identified.

An Optical Flow technique based on the use of Dynamic Programming has been successfully applied to Particle Image Velocimetry yielding a significant increase in the accuracy and spatial resolution.

In the future we have to develop a technique of vortices extraction in order to characterise their time and spatial dynamics. The height optical flow resolution coupled with a PIV 3D velocity measurements will permit to better characterise the Reynolds tensor and valid the viscosity models used in the LES simulation.

REFERENCES

[1] J.B. Wedding, D. Lombardi and J. Cermak: J. Air Pollut. Control Ass, **27**, 557-566 (1977):

[2] F. T. DePaul and C.M. Sheih: Atmospheric Environment **20**, 455-459 (1986),.

[3] D.A. Paterson and C.J. Apelt: Bldng. Envir, **24**, 39-50 (1989)

[4] G.M. Quénot: ‘The Orthogonal Algorithm for Optical Flow detection using Dynamical Programming’In: *Proc. IEE ICASSP*, *San Francisco, (1992)*, vol. 3, pp. 249-252

[5] A. Chabni: ‘Etude par méthodologie de type Simulation des Grosses structures de la dynamique de l’interaction et des échanges entre une couche limite et une encoche’, Thèse de l’Université Paris XI, 1997.